Journal of Chromatography A, 1457 (2016) 41–49

Contents lists available at ScienceDirect

Journal of Chromatography A

journal homepage: www.elsevier.com/locate/chroma

Simulation of elution profiles in liquid chromatography—I: Gradient elution conditions, and with mismatched injection and mobile phase solvents

Lena N. Jeong [a], Ray Sajulga [b], Steven G. Forte [a], Dwight R. Stoll [b,*], Sarah C. Rutan [a,*]

[a] Department of Chemistry, Virginia Commonwealth University, 1001 W. Main St., Richmond, VA 23284-2006, USA
[b] Department of Chemistry, Gustavus Adolphus College, 800 W. College Ave., Saint Peter, MN 56082, USA

ARTICLE INFO

Article history:
Received 18 October 2015
Received in revised form 19 May 2016
Accepted 5 June 2016
Available online 6 June 2016

Keywords:
Sample/eluent solvent mismatch
Sample volume overload
Linear solvent strength theory
Simulation

ABSTRACT

High-performance liquid chromatography (HPLC) simulators are effective method development tools. The goal of the present work was to design and implement a simple algorithm for simulation of liquid chromatographic separations that allows for characterization of the effect of injection solvent mismatch and injection solvent volume overload. The simulations yield full analyte profiles during solute migration and at elution, which enable a thorough physical understanding of the effects of method variables on chromatographic performance. The Craig counter-current distribution model (the plate model) is used as the basis for simulation, where a local retention factor is assigned for each spatial and temporal element within the simulation. The algorithm, which is an adaptation of an approach originally described by Czok and Guiochon (Ref. [10]), is sufficiently flexible to allow the use of either linear (e.g., Linear Solvent Strength Theory) or non-linear models of solute retention (e.g., Neue-Kuss (Ref. [36])). In this study, both types of models were used, one for simulating separations of a homologous series of alkylbenzenes, and the other for separations of selected amphetamines. The simulation program was validated first by comparison of simulated retention times and peak widths for five amphetamines to predictions obtained using linear solvent strength (LSS) theory, and to results from experimental separations of these compounds. The simulated retention times for the amphetamines agreed within 0.02% and 2.5% compared to theory and experiment, respectively. Secondly, the program was evaluated for simulating the case where there is a compositional mismatch between the mobile phase at the column inlet and the injection solvent (i.e., the sample matrix). This work involved alkylbenzenes, and retention time and peak width predictions from simulations were within 1.5 and 6.0% of experimental values, respectively, even without correction for extra-column dispersion. The issues of sample/eluent solvent mismatch and solvent volume overload are especially important when considering the challenges of transferring eluent from the first to the second dimension in comprehensive two-dimensional liquid chromatography.

1. Introduction

The method development process in HPLC involves optimization of method parameters such as stationary phase, column dimensions, initial and final mobile phase compositions, as well as gradient time when gradient elution is used [1]. Computer simulation can aid in the optimization of separation methods, which can save time as compared to trial-and-error approaches [1–9]. In the past, several different methods for solving the mass transport equations defining the evolution of chromatographic peaks have been used including the Craig distribution model (based on the concept of theoretical plates) and mass balance equations (based on obtaining elution profiles through numerical integration) [10–18]. There are also several commercially available simulation software packages that use linear solvent strength (LSS) theory or linear free energy-type relationships such as DryLab (Molnar-Institute) [2,3,6,19], LC&GC Simulator (ACD/Labs) [9,20] and ChromSword Offline (Merck KGaA) [5,21]. The ChromSword offline program builds a physico-chemical retention model based on the structural formulae of the compounds, the type of column, and the type of organic solvent [5]. The simulation result achieved by this method of retention modeling becomes the initial starting point for method optimization. The ACD/Labs package uses either a database of experimental chromatograms or physico-chemical

* Corresponding authors.
E-mail addresses: dstoll@gustavus.edu (D.R. Stoll), srutan@vcu.edu (S.C. Rutan).

http://dx.doi.org/10.1016/j.chroma.2016.06.016
0021-9673/

parameters to model chromatograms and to predict optimal separation conditions. DryLab predictions are based on LSS theory and are initiated solely by experimental data obtained from training separations [22,23]. Kaliszan et al. compared the performance of two of these programs and concluded that structure-based predictions by ChromSword offline were less accurate compared to retention measurement-based simulation of DryLab [6,24]. The limitations of these methods result from the lack of flexibility in modeling unusual gradient shapes and realistic injection profiles. As an example, these methods do not allow for the characterization of the effect of solvent mismatch between the sample solvent and the eluent, which is a major focus of the present work.

A number of reports in the literature have described methods for chromatographic simulations using a variety of numerical methods to solve the mass transport equations [7,11–13,15,17,18,25–29]. These methods vary in terms of accuracy, speed and complexity. In this paper we present a general simulation program to predict the results of HPLC separations using a Craig-type simulation where the analyte propagates through a discretized space and time grid [7,10]. While this algorithm can be slow because of the necessity of calculating results at each point in time and space, it is relatively simple to understand and as we will show, produces results that agree well with closed form theory. Our program incorporates pre-elution of weakly retained compounds before the gradient reaches the head of the column. In addition, it can be easily adapted to any eluent composition profile (not just a linear profile), any stationary phase composition (constant or non-constant), and any composition and shape of the injected sample profile. Therefore, these simulations can be particularly useful in characterizing the solvent mismatch effect in comprehensive two-dimensional liquid chromatography, where sample solvent frequently differs in organic strength or polarity and causes peak distortion (broadening) [30–32]. Finally, the evolution of the chromatogram can be captured in the form of movies and/or snapshots of the analyte distribution over time and/or distance to facilitate a better understanding of the separation process under complicated circumstances.

It is important to note that in this work we use LSS or Neue-Kuss theory to obtain parameters that should be able to predict retention for all mobile phase compositions on the corresponding stationary phase. Then, in principle, we can use any type of mobile phase gradient or injection solvent mismatch profile we like, hence being able to explore many conditions not explicitly described by closed-form theory. However, in the present paper, much of what we are trying to do is to demonstrate that the code we have developed is valid, and we show this by demonstrating the very close agreement between closed-form equations and simulations. Then, in subsequent work, we can explore all sort of unusual phenomena not explained by closed form theory.

2. Theory

All symbols and variables are defined in a Glossary provided in the Supplemental material.

2.1. Craig distribution model for isocratic, isothermal chromatography

The Craig model explains the chromatographic process as a series of pseudo counter-current distributions between two immiscible liquids [10]. In this model, the sample mixture is introduced into liquids with different densities and undergoes equilibration between the two phases. The mobile phase is moved to the next tube while fresh mobile phase is introduced into the first tube. Equilibration occurs in each tube and the concentration of solute in the last tube is monitored. This concept can be applied to chromatography by dividing the column into discrete distance segments to represent tubes. This is one of the simplest, yet physically reasonable finite-difference strategies for the numerical solution of the differential equation shown by eq. A1 (see Appendix). According to Czok and Guiochon, the Craig distribution model can be used to explain the continuous chromatographic process by replacing a column with segments of length (Δz) and time (Δt) in a grid [10]. Here, we assume Δz is equal to the plate height (H) for the chromatographic system under study. As shown in Fig. 1, at every time interval, part of the analyte mass from initial position, z-1, travels to the next cell downstream (z, t), while the remaining mass stays at the initial position, (z-1, t). The fraction of mass that travels to the next position in the column (z, t) is equal to μ, which is the peak velocity normalized to mobile phase velocity or simply the solute mobility, where k is the chromatographic retention factor (see Eq. (1)).

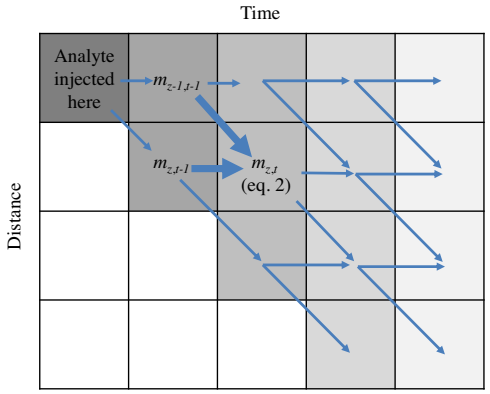

Fig. 1. Propagation of the analyte through a time-distance grid in the Craig distribution model. Adapted from Ref. [10].

$$\mu = \frac{1}{k+1} \tag{1}$$

Alternatively, one can view μ as the fraction of analyte in the mobile phase, while 1-μ represents the fraction remaining in the stationary phase, which is also called the analyte immobility,ω. The analyte mass is moved from one cell to the next, one step at a time. Therefore, the mass (m) at particular position (z) and at time (t) can be calculated using Eq. (2);

$$m_{z,t} = \omega m_{z,t-1} + \mu m_{z-1,t-1} \tag{2}$$

Finally, the last row of the grid (where z equals the column length, L) contains the numerical mass of analyte that has exited the column as a function of time – in other words, plotting the masses at $z = L$ as a function of time gives the analyte elution profile, or the chromatogram, that we are most familiar with.

2.2. Linear solvent strength (LSS) theory

2.2.1. Retention time prediction

According to the LSS model of Snyder et al., the retention of an analyte separated under conditions where a linear mobile phase gradient is used can be predicted based on measurements of isocratic retention factor (k) as a function of solvent concentration (ϕ) [22].

$$\ln k = \ln k_w - S\phi \tag{3}$$

where S is the slope of a plot of isocratic ln k values versus ϕ, and k_w is the retention factor for the solute in a purely aqueous phase.

The analyte retention time (t_R) under gradient elution conditions can be predicted using the LSS model, which includes a

pre-elution phase that exists when there is a non-zero gradient delay time (t_D) [22,33,34]:

$$t_R = \left(\frac{t_M}{b}\right) \ln\left\{k_o b\left(1 - \frac{t_D}{t_M k_0}\right) + 1\right\} + t_M + t_D \quad (4)$$

here, t_M is the void time and k_0 is the initial retention factor at the start of the gradient, calculated as $k_0 = k_w e^{-S\phi}$, and b is the intrinsic, dimensionless gradient steepness that can be expressed as

$$b = \frac{V_M \Delta\phi S}{t_G F} = \frac{t_M \Delta\phi S}{t_G} \quad (5)$$

If a linear gradient is simulated with the Craig model using the assumptions of LSS, the closed form expression given in Eq. (4) can be used to validate the retention times of the analyte obtained by the simulation code.

In order to ensure the mass balance conservation for the gradient chromatography simulations (where the retention factor k depends on both time and position), the mass profile equation must be derived from the time and distance dependent retention factor k (see Appendix A). The following equation (Eq. (6)) differs from the equation given by Czok and Guiochon due to the fact that the analyte velocity is dependent on position inside the column. According to Blumberg [48], the velocity of the analyte, not just its dispersion, must be a function of position to ensure mass conservation of a gradient system. Therefore, the differential of analyte velocity must be taken over the position (see Appendix A).

$$m_{z,t} = m_{z,t-1}\omega_{z,t-1} + m_{z-1,t-1}\mu_{z-1,t-1} \quad (6)$$

A shortcoming of the Craig model is that it does not accurately account for peak broadening. However, as mentioned by Czok and Guiochon [10], this can be addressed empirically by assuming that the extra peak broadening can be treated as a dispersion process where the extent of the dispersion is estimated using Fick's second law. The additional dispersion (D_z) each peak experiences depends on the local retention factor [10,23,35]. Fick's second law states the following

$$\frac{\partial m}{\partial t} = D_z \frac{\partial^2 m}{\partial z^2} \quad (7)$$

Or, in other words, the analyte at position $m_{z,t}$ is redistributed to the previous, current, and next positions to simulate kinetic broadening of the analyte zone:

$$\frac{m_{z,t+1} - m_{z,t}}{\Delta t} = D_z \frac{m_{z+1,t} - 2m_{z,t} + m_{z-1,t}}{\Delta z^2} \quad (8)$$

The effective dispersion coefficient, D_z, is calculated at the local k value [10]:

$$D_z = \frac{1}{2(k_{z,t-1} + 1)^2} \frac{\Delta z^2}{\Delta t} \quad (9)$$

Note that in the present work we have assumed that the Δz is constant along the column length. In gradient separations, the peak width (determined by the efficiency) is linked to the choice of Δz. The effect of the change of analyte velocity during the course of the mobile phase gradient is captured by Eq. (9) by adjusting the peak width according to the local retention factor. The more subtle effect on the plate height caused by changes in the analyte diffusion coefficient in the mobile phase, as the mobile phase composition varies, is not accounted for here.

In order to accurately assess the degree of band broadening, the mass of solute present at position, z, and time, t, along the column is first determined using Eq. (6), and then Eq. (8) is used to add the additional broadening by adding the following differential mass to $m_{z,t}$:

$$m_{z,t+1} - m_{z,t} = D_z \frac{\Delta t}{\Delta z^2}\left(m_{z+1,t} - 2m_{z,t} + m_{z-1,t}\right) \quad (10)$$

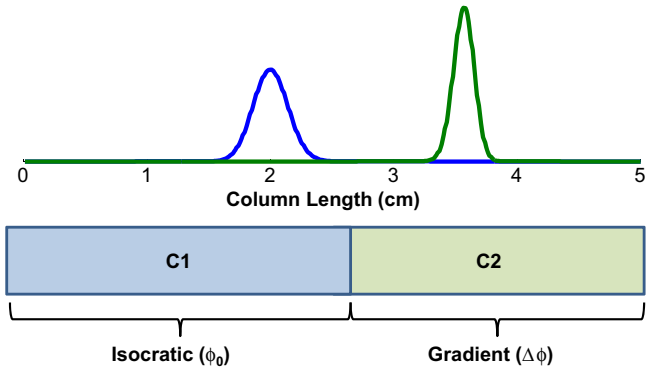

Fig. 2. Simulation of an analyte with high initial retention factor under conditions where there is a significant gradient delay, t_D. The total column length = C1 + C2. During the gradient delay time, the analyte experiences isocratic condition (C1), whereas a changing solvent strength is experienced when the mobile phase gradient catches up with the analyte (C2). Simulation conditions: $\Delta z = 0.01$ cm; $\Delta t = 0.06$ s; $\phi_o = 0.02$; $\Delta\phi = 0.8$; $k_w = 100$; S = 100; $t_G = 5$ min; $t_D = 3.5$ min; $L = 5$ cm. Under these conditions, the gradient catches up with the analyte peak after 3.76 min, at a distance 2.59 cm down the column. The profile at 2 cm occurs at 2.9 min and the profile at 3.9 cm occurs at 4.1 min.

This results in the final simulated chromatogram exhibiting a peak width corresponding to $H = \Delta z$. Finally, because the amount detected by the detector, m_d, is the analyte mass in the mobile phase, the simulated total mass profile ($m_{L,t}$) has to be corrected using the retention factor at the elution point, k_e (see Appendix A, Eqs. (A8) and (A9)). If this is not done, the area of the peak at the column outlet is dependent on retention factor, which is physically unreasonable.

$$m_d = \frac{m_{L,t}}{1 + k_e} \quad (11)$$

2.2.2. Peak width prediction

The widths of simulated peaks can be validated by considering the effect of a negative solvent strength gradient through the column on peak widths [22]. In the case of a significant gradient delay time, the analyte experiences an isocratic mobile phase during its travel through the first section of the column (C1 in Fig. 2), followed by a solvent of changing composition as it travels through the rest of the column (C2). Therefore, one can view the broad peak from section C1 as a non-ideal sample injection into section C2. The total peak variance is the sum of the variance that develops in section C2 (σ^2_{grad}) and the variance developed during travel through C1 ($\Delta\sigma^2_{iso}$). The increase in solvent strength over time at all positions in the column under gradient conditions accelerates band migration, resulting in a substantial decrease in the peak retention times and widths [23,32]. In addition to that, the front of the band moves slower than its tail, resulting in relatively minor additional peak width reductions [32]. The gradient band compression factor describing this effect can be written as

$$G_{bR} = \frac{1}{1 + b^*\omega_0}\sqrt{1 + b^*\omega_0 + \frac{1}{3}b^{*2}\omega_0^2} \quad (12)$$

where the fraction of solute in the stationary phase at the beginning of the gradient is indicated as ω_0 (solute initial immobility). The fraction of solute in the mobile phase (solute mobility) as the band elutes (μ_R) can be expressed in terms of ω_0 and the dimensionless gradient steepness (b*) [35]:

$$\omega_0 = \frac{k_0}{k_0 + 1} \quad (13)$$

$$\mu_R = 1 - \frac{\omega_0}{\omega_0 b^*} \quad (14)$$

The peak width developed due to injecting a finite bandwidth (σ_b) onto the column can be calculated as [35]:

$$\Delta\sigma_{iso} = \frac{t_M \sigma_b}{L\mu_R(1 + b^*\omega_0)} \quad (15)$$

The dimensionless gradient slope, b^*, is only applicable over the section of the gradient that the analyte experiences. Therefore, the void time used in this equation must be a fractional t_M (*i.e.*, $t_{M,grad}$) for the gradient section only:

$$b^* = \frac{t_{M,grad}\Delta\phi S}{t_G} \quad (16)$$

$$\sigma_{grad} = \frac{G_{bR} t_{M,grad}}{\mu_R}\sqrt{\frac{\Delta z}{L_{grad}}} \quad (17)$$

The total peak variance on column when there is significant pre-elution caused by a finite t_D is finally calculated as

$$\sigma^2_{col} = \Delta\sigma^2_{iso} + \sigma^2_{grad} \quad (18)$$

2.3. Non-LSS theory gradient retention model (Neue and Kuss)

An alternative description of the retention factor dependence on the mobile phase composition has been proposed by Neue and Kuss, which takes into account the fact that the variation of the logarithm of retention factor as a function of the solvent strength is actually nonlinear and has a curved relationship [36,37]:

$$k = k_w(1 + S_2\phi)^2 \exp\left[\frac{-S_1\phi}{1 + S_2\phi}\right] \quad (19)$$

where S_1 and S_2 are parameters describing the slope and the curvature of the ln k vs. ϕ plot, respectively. The parameters k_w, S_1 and S_2 can be extracted by fitting experimental retention factors from isocratic elution experiments to Eq. (19), and then retention times can be predicted using

$$t_R = \frac{t_G(\phi_e - \phi_0)}{\Delta\phi} + t_M + t_D \quad (20)$$

where the organic composition at elution (ϕ_e) can be expressed as [37,38]:

$$\phi_e = \frac{\phi_0 + \frac{1+S_2\phi_0}{S_1}\ln\left(\frac{\Delta\phi k_w S_1}{t_G}\left(t_M - \frac{t_D}{k_0}\right)\exp\left(\frac{-S_1\phi_0}{1+S_2\phi_0}\right) + 1\right)}{1 - \frac{S_2(1+S_2\phi_0)}{S_1}\ln\left(\frac{\Delta\phi k_w S_1}{t_G}\left(t_M - \frac{t_D}{k_0}\right)\exp\left(\frac{-S_1\phi_0}{1+S_2\phi_0}\right) + 1\right)} \quad (21)$$

(The interested reader should note that this equation is given in the supporting material of reference [37] as Eq. S21.) The extracted Neue-Kuss parameters can also be used to calculate retention times and peak widths in simulations of mobile phase gradients with or without sample/eluent solvent mismatch conditions.

2.4. Sample/eluent solvent mismatch theory

2.4.1. Peak width prediction

The width of peaks injected under conditions of sample volume overload with a mismatched sample solvent can be estimated using a similar analysis to that used to estimate the peak width under gradient conditions. The total peak width (σ_{tot}) can be described as the combination of peak width caused by the column (σ_{col}) and the broadening ($\Delta\sigma_{inj}$) caused by non-ideal sample injection.

$$\sigma^2_{tot} = \sigma^2_{col} + \Delta\sigma^2_{inj} \quad (22)$$

There is a deviation in peak variance due to the injected sample when the composition of the sample solvent and mobile phase is different and the sample volume is large. This variance due to the injected sample/eluent solvent mismatch and sample volume overload can be estimated as follows [39]

$$\Delta\sigma^2_{inj} = \left[\frac{k_{mp} + 1}{k_{ss} + 1}\right]^2\left[1 + \frac{k_{mp} - k_{ss}}{k_{ss} + k_{ss}k_{mp}}\right]^2\left(\frac{V^2_{inj}}{12F^2}\right) \quad (23)$$

where k_{mp} and k_{ss} are the retention factors of the analyte in the mobile phase and the sample solvent, respectively, and V_{inj} and F are injection volume and flow rate, respectively. This equation is obtained by simplification of the expression given by Raglione et al. for a system comprised of an analytical column coupled to an accelerator column [39]. This equation can be simplified further to give

$$\Delta\sigma^2_{inj} = \left(\frac{k_{mp}}{k_{ss}}\right)^2\left(\frac{V^2_{inj}}{12F^2}\right) \quad (24)$$

which assumes a rectangular injection pulse. The contribution to the total peak variance due to dispersion inside the column is calculated from the expected plate number (N) and retention time (t_R):

$$\sigma^2_{col} = \frac{t^2_R}{N} \quad (25)$$

It should be noted that when the injection peak width is larger than the column peak width, as in the case of sample/eluent solvent mismatch and injection volume overload conditions, the resulting peak is not Gaussian. Therefore, the retention time and peak variance cannot be reliably estimated from the max position and full width at half maximum, which are based on the assumption of a Gaussian peak shape. The correct retention time and peak variance must be calculated using the first and second central moment of the peak, respectively.

3. Experimental

3.1. Isocratic experiments

Isocratic retention data were collected for the alkylbenzenes methylbenzene (AB1), ethylbenzene (AB2), propylbenzene (AB3), butylbenzene (AB4), and pentylbenzene (AB5) using a system composed of a binary pump, autosampler, column thermostat, and diode-array UV detector, all from the 1290 Infinity series from Agilent Technologies (Santa Clara, CA). The column used for this experiment was Zorbax Stablebond C_{18} (50 × 4.6 mm, 3.5 μm, Agilent). This specific column and particle size was selected so that measured peak variances would be minimally affected by peak dispersion outside of the column. Retention times were measured at 40 °C in mobile phases between 10% and 90% (v/v) acetonitrile (ACN) in steps of 10% for solute/eluent pairs that gave retention factors less than 50. The column dead volume was measured using uracil in a mobile phase of 50/50 ACN/water, and the extra-column volume was determined under the same conditions, but with the column replaced with a zero dead volume union. The Neue-Kuss parameters were extracted from this data set by fitting to Eq. (19), and the resulting parameters are given in Table S1 of the Supplemental Material. These parameters were used to simulate both isocratic (see Section 4.3) and gradient (see Section 4.1) separations of the alkylbenzenes, and the retention times and peak widths resulting from simulations of gradient separations of the alkylbenzenes were then compared to experimental results.

3.2. Gradient experiments

Gradient elution separations of alkylbenzenes were carried out using the Agilent 1290 Infinity system and Stablebond C_{18} column

described above in Section 3.1. The flow rate was 2.0 mL/min, the column temperature was 40 °C, the injection volume was 1 μL, and a gradient from 50 to 90% ACN over 2.25 min was used for elution.

A group of five amphetamines was selected to characterize the performance of simulations of gradient elution separations. The structures, names, and abbreviations for these compounds are shown in Fig. S1. The gradient data were collected on a system composed of binary pump, autosampler, column thermostat, and diode array detector (DAD) from the HP 1090 system (Agilent). The column was an Accucore Phenyl-Hexyl column (100 × 2.1 mm, 3 μm, Thermo Scientific), and the mobile phases were 10 mM potassium phosphate buffer at pH 2.5 and ACN. The S and k_w values were estimated using nonlinear least squares regression using Eqs. (4) and (5) and fitting to the different experimental gradient retention times as a function of the gradient times (t_G) and initial mobile phase compositions (ϕ_o). These S and k_w values were used to simulate the retention of amphetamines under various gradient conditions, and these parameters are given in Table S2 of the Supplemental Material. The retention times and peak widths resulting from simulations of gradient elution separations of these compounds were compared to both predictions based on LSS theory, and to experimental results.

3.3. Sample/eluent solvent mismatch experiments

A second set of experimental data (retention times and peak widths) was collected for the alkylbenzenes under isocratic conditions, where the initial mobile phase and injection solvents were different (i.e., 'solvent mismatch' conditions). In this case a system composed of a pump and autosampler from the HP1050 series (Agilent), and column thermostat and diode-array UV detector from the Agilent 1100 series was used. This particular system was chosen for this experiment because the autosampler is equipped with a syringe and sample loop that allows injections of up to 100 μL. The Neue-Kuss parameters extracted previously (see Section 3.1) were used to simulate separations under sample/eluent solvent mismatch conditions, and the resulting retention times and peak widths were compared to experimental results.

3.4. Simulation codes

All simulation codes were written in the Matlab program (Mathworks, Natick, MA) version R2013a. Non-linear regression to obtain the parameters necessary to implement simulations was accomplished using the function lsqnonlin found in the Matlab Optimization Toolbox. The simulation codes are currently under development and are available to interested users upon request.

4. Results and discussion

4.1. Prediction of alkylbenzene retention under gradient elution conditions using Neue-Kuss parameters determined from isocratic retention data

Simulation of gradient elution separations of alkylbenzenes were performed using the extracted Neue-Kuss parameters and plate numbers shown in Table S1, assuming a linear change in solvent composition with time. Fig. 3 shows a qualitative comparison of experimental and simulated chromatograms collected for gradient separations of alkylbenzenes AB1-5 for a solvent gradient with a ϕ_o of 0.50 and a $\Delta\phi$ of 0.40 over a t_G of 2.25 min. Table 1 summarizes the comparison of experimental and simulated retention times and peak widths. Predicted retention times were accurate to within 1.5%, and predicted peak widths were accurate to within 6.0%. The simulated data compare well with the experimental data even though no correction of the simulated results has been made to account for increases in retention time and peak dispersion caused by extra-column volume.

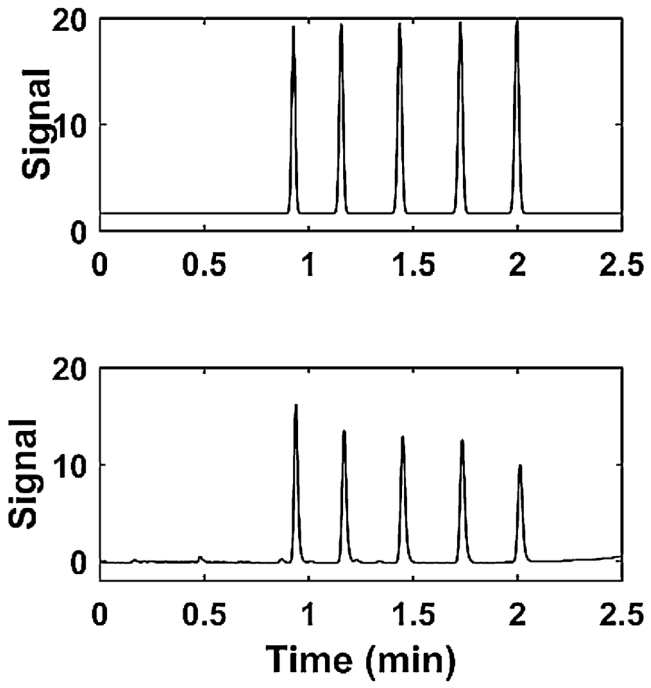

Fig. 3. Experimental (bottom) and simulated (top) chromatograms collected for gradient separations of alkylbenzenes AB1-5. The solvent gradient was 50–90% ACN from 0 to 2.25 min, and injection volume was 1 μL. The measured gradient delay time of 0.055 min was used in the simulation.

4.2. Prediction of amphetamine retention under gradient elution conditions using LSS parameters determined from gradient retention data

The Neue-Kuss parameters could not be extracted from the gradient experimental data for the amphetamine-class compounds since the system is ill-conditioned. This was because a limited experimental data set was available. This means that a wide range of Neue-Kuss parameters predicted experimental gradient retention times with very similar values. For gradients with shallower slopes, the linear model resulted in better predictions [37]. Therefore, the linear parameters S and k_w were extracted from the gradient data for the amphetamine-class compounds. The simulation results were then validated with LSS theory, as discussed below. The simulated results were also compared to the experimental data, and these comparisons are also shown in Fig. 4 and Table 2. The retention time predictions agreed to within 2.5%. The experimental peak width comparisons are also quite reasonable. This level of agreement indicates that the LSS model for these parameters is adequate for generating reasonable predictions for retention behavior.

4.3. Sample/eluent solvent mismatch experiments

There is a great interest in the peak distortion caused by a difference in the solvent composition of the sample and the eluent used in an LC method [31,40–44]. This may result from low solubility of the analyte in water, or be a consequence of other method development decisions in two-dimensional liquid chromatography (2D-LC). This is particularly problematic when the eluent from the first dimension contains more organic solvent than the initial eluent composition in the second dimension of 2D-LC under

Table 1
Experimental and simulated retention data for AB1-5 separated under gradient elution conditions[a].

Solute	Retention Time (min)		Peak Width ($w_{1/2}$, min)	
	Experiment	% Difference (Simulation – Experiment)[b]	Experiment	% Difference (Simulation – Experiment)[b]
AB1	0.939	−1.3	0.0198	−4.9
AB2	1.169	−1.2	0.0217	−4.9
AB3	1.451	−1.0	0.0233	−5.3
AB4	1.736	−0.5	0.0242	−5.7
AB5	2.012	−0.8	0.0244	−5.8

[a] The solvent gradient was 50–90% ACN from 0 to 2.25 min, and the injection volume was 1 μL. The measured gradient delay time of 0.055 min and a rectangular injection profile were used for the simulations.
[b] % difference = $^{(sim - exp)}/_{exp}$.

Table 2
Comparison of retention time and peak width prediction of simulation, LSS and experiments for amphetamines[a].

Solute	Retention Time (min)			Peak Width ($w_{1/2}$, min)		
	LSS[b]	% Difference (Simulation – LSS)[c]	% Difference (Simulation – Experiment)[d]	LSS & Simulation[e]	% Difference (Simulation – LSS)[c]	% Difference (Simulation–Experiment)[d]
Amp	2.6741	−0.016	1.49	0.1089	−0.017	7.51
MDMA	3.7052	−0.018	1.96	0.1250	−0.011	−12.9
MDE	4.7021	−0.019	2.20	0.1430	−0.0074	21.2
Bromo	7.6523	−0.017	1.07	0.1882	−0.00036	46.5
BP	10.9164	−0.014	0.51	0.2091	−0.0050	41.0

[a] The solvent gradient was 5–35% ACN from 0 to 18 min. The measured gradient delay time of 0.795 min and a rectangular injection profile were used for the simulations.
[b] Calculated using Eqs. (4)–(5).
[c] %difference = $\frac{(sim-LSS)}{LSS}$.
[d] %difference = $\frac{(sim-exp)}{exp}$.
[e] Calculated using Eqs. (12)–(18).

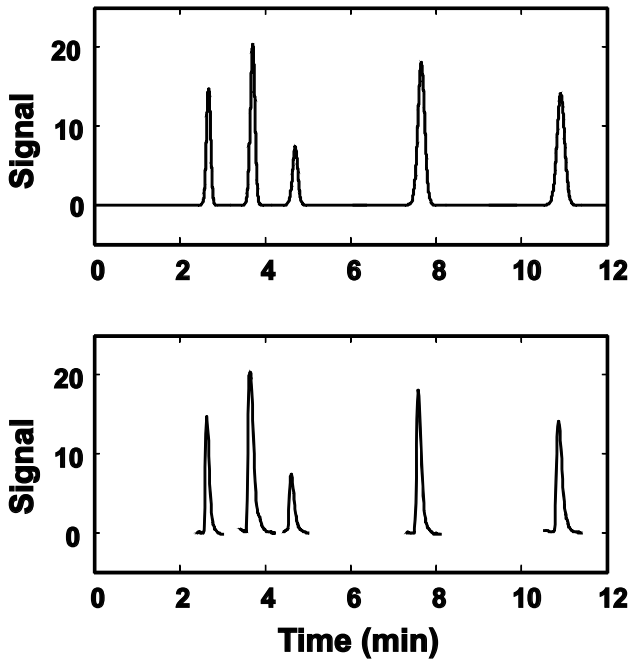

Fig. 4. Experimental (bottom) and simulated (top) chromatograms collected for gradient separations amphetamines. The solvent gradient was 5–35% ACN from 0 to 18 min. The measured gradient delay time of 0.795 min was used in the simulation. The simulations are scaled to the intensity of the experimental chromatograms. The gaps in the baseline of the experimental chromatograms are due to the fact that the compounds were injected in different samples.

reversed-phase conditions [43–47]. Sample volume overload can also produce problematic peak shapes [42,48,49].

In 2D-LC the first dimension (^{1}D) effluent can be diluted to be more similar to the starting solvent composition when gradient elution is used in the second dimension. However, there are practical limits to how much the ^{1}D effluent can or should be diluted [47]. Given the complexity associated with optimizing these conditions, it is of great interest to accurately simulate such large volume injection conditions to give a better understanding of analyte behavior under these conditions. Here, we investigate these effects under isocratic conditions, in which the retention times and peak widths are very sensitive to the volume and composition of the sample. Figs. 5–7 show comparisons of results obtained from experiments, simulations, and predictions based on theory.

Fig. 5 shows a qualitative comparison of experimental and simulated chromatograms obtained for isocratic separations at 70/30 ACN/water of alkylbenzenes AB1, AB3, and AB5 in samples with varying solvent composition. Simulations were based on rectangular injection profiles. The retention times, widths, and shapes of the simulated peaks are consistent with those observed in experiments. Figs. 6A and B show comparisons of retention times extracted from the experimental or simulated chromatograms across the variable space studied (1–100 μL injection volume; 50 or 90% ACN sample solvent). We do not show results for retention times calculated from theory in this figure, because no satisfactory closed form theory for this effect has been proposed in the literature. Fig. 6A shows data for methylbenzene (AB1, k = 1.67) and 5 B shows data for pentylbenzene (AB5, k = 7.81) when injected from samples containing either 50 or 90% ACN. These figures show that retention times shift later with increasing volume of sample containing less ACN compared to the mobile phase, and shift to earlier times when increasing volume of sample containing more ACN compared to the mobile phase is injected. This observation is as expected since the analyte peak elutes faster at the higher concentration of organic solvent, and the simulations accurately capture this effect.

The peak shape is also distorted when the injection and eluent solvents are mismatched [43]. As mentioned before, this peak distortion is more pronounced when the injection solvent is stronger than the eluent solvent. The peak widths measured from simulations were validated by comparison with theoretical peak width calculations (Eqs. (22)–(25)). As shown in Fig. 7B, as the sample

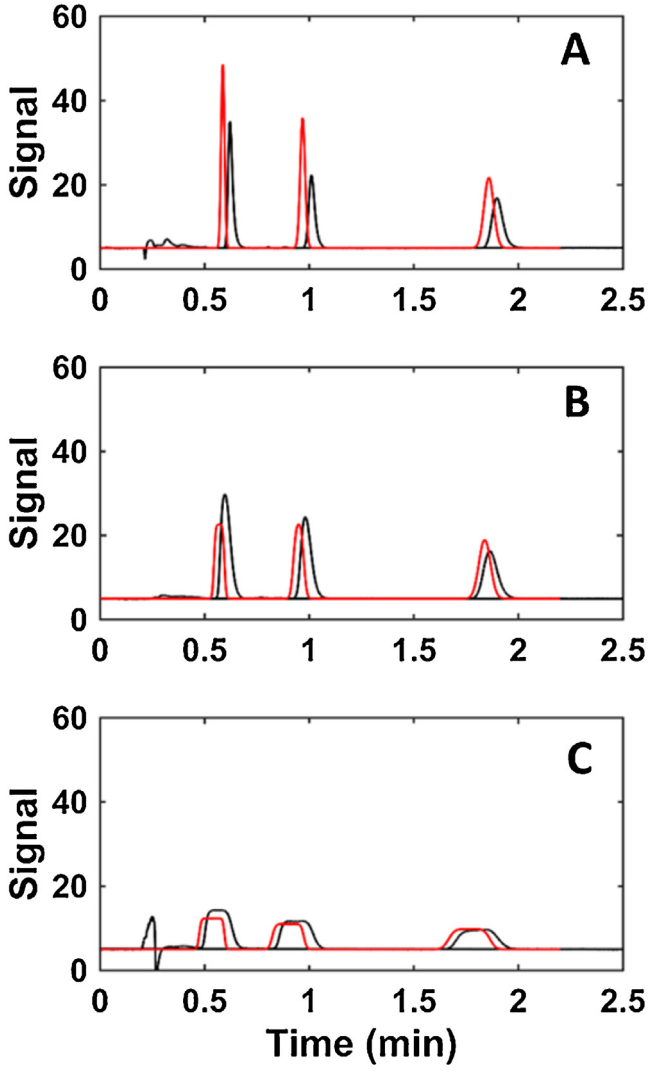

Fig. 5. Experimental (black) and simulated (red) chromatograms collected for isocratic separations of alkylbenzenes AB1 (first peak), AB3, and AB5 (last peak). The eluent was 70% ACN, and injection volume was 100 μL. Sample solvents were 50 (A), 70 (B), or 90 (C) % ACN.

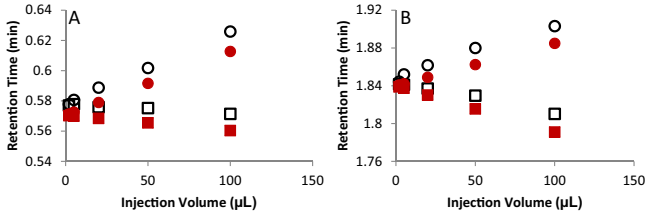

Fig. 6. Comparison of experimental (black, open symbols) and simulated (red, closed symbols) retention times for sample/eluent solvent mismatch. Retention times for (A) methylbenzene ($k = 1.67$) and (B) pentylbenzene ($k = 7.81$) injected from either 50% (circles) or 90% (squares) ACN samples into an eluent containing 70% ACN. The percent difference between the experimental and simulated retention times was within 2.2% for AB1 and within 1.0% for AB5.

injection volume increases, the peak tends to get broader due to the initial solute elution in the injection solvent before the peak is slowed down by weaker solvent. This peak broadening effect does not exist for samples with the weaker injection solvent due to the focusing achieved in the stronger mobile phase (Fig. 7A). We attribute the slightly larger widths measured in experiments (Fig. 7A) to peak tailing that is not accounted for in the simulations

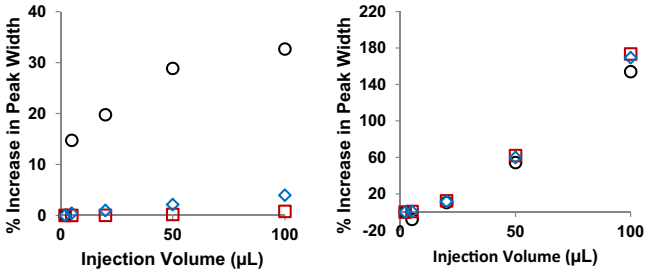

Fig. 7. Percent increase in peak width for pentylbenzene (AB5) as a function of injection volume. Samples are in (A) 50% and (B) 90% (v/v) ACN for an eluent containing 70% (v/v) ACN. Black open circles are experimental, red open squares are for simulation and blue open diamonds are for theory (Eqs. (22)–(25)).

or predictions from theory, as well as the fact that the theory is only approximate. This is a subject of ongoing work that we will address in detail in a subsequent manuscript. Briefly, we now believe that most of the tailing observed in this case originates from the asymmetric profile of the injected sample as it exits the injection system and enters the column. The simulations carried out as described here have assumed that the sample enters the column as a perfectly rectangular pulse. Subsequent work will show that when an asymmetric profile that accurately reflects the way the sample actually enters column is used to introduce analyte mass into the simulated column the simulation produces tailed peaks that are more consistent with experimental results.

5. Conclusion

A finite difference scheme, based on the Craig model of chromatography, has been developed to solve the partial differential equations defining chromatographic elution for some specific systems of interest. It enables simulation of chromatographic peaks eluted under gradient or isocratic conditions where the mobile phase and sample solvents are not matched. The analyte mass propagation down the column was calculated using estimates of local retention factors at regular spatial increments as the solute zone progresses along the column, as time increases. The approach is similar to that proposed by Czok and Guiochon [10] with an important distinction. The equations for non-steady state conditions in the original paper (applied to Langmuir isotherms) were in error and are corrected here and applied to both gradient mobile phase conditions and non-ideal injection conditions, which were not discussed in the original paper. It should be pointed out, however, that a different strategy might need to be developed for compressible mobile phases, because in that case the mobile phase velocity is not constant, and varies over the column length. This would be useful for addressing sample/eluent solvent mismatch issues in supercritical fluid chromatography [50–52]. In addition, it might be useful to develop a more general method to account for the possible time and distance dependence of the dispersion.

In this work, we have shown that both linear (LSS) and nonlinear (Neue-Kuss) solvent strength models can be used to provide retention factors for the simulations. The accuracy of the simulation code was validated against LSS theory. The retention times obtained by simulation compared well to experimental results as well. Under sample/eluent solvent mismatch conditions, the expected retention time trend was confirmed and the increases in the simulated peak widths were validated against predictions from theory. This use of this simulation program can facilitate a deeper understanding of liquid chromatography and the development of new LC methods by reducing time-consuming trial-and-error experiments.

In order to provide a more flexible and powerful simulator that can be used by analytical chemists to facilitate method develop-

ment, we anticipate the following developments in subsequent work: 1) add accounting for analyte mass overload (e.g., Langmuir isotherm) by utilizing an inverse method for isotherm parameter extraction [53,54]; 2) application to segmented gradients; 3) automated simulation of random combinations of operating conditions (Monte-Carlo); 4) simulation of linear and exponential stationary phase gradients [55]; and 5) algorithm and code optimization for rapid computation and discovery of optimal conditions.

Acknowledgements

DRS would like to thank the Camille and Henry Dreyfus Foundation Faculty Teacher-Scholar Program for supporting this work. DRS and RS have also been supported by grants from the National Science Foundation (CHE-1213244 and CHE-1508159). Some of the experimental data were obtained using instrumentation on loan from Agilent Technologies. SCR, SGF and LNJ acknowledge support from the National Science Foundation (CHE-1213364 and CHE-1507332). The authors would also like to acknowledge the constructive comments from several helpful reviewers during the review process.

APPENDIX A Derivation of Craig model for time and distant dependent retention factors

According to Blumberg [56,57], the change in total mass of an analyte in a non-uniform medium (i.e., a gradient) along the time domain can be expressed as the following differential equation with the analyte velocity and its dispersion both as functions of position

$$\frac{\partial m}{\partial t} = \frac{\partial^2}{\partial z^2}(Dm) - \frac{\partial}{\partial z}(u_a m) \tag{A1}$$

where m is the mass of analyte per unit length, t is time, z is distance, D is diffusivity and u_a is the analyte velocity. With the assumption of no diffusion, the equation is simplified to

$$\frac{\partial m}{\partial t} + \frac{\partial}{\partial z}(u_a m) = 0 \tag{A2}$$

where $u_a = u_m/(1+k)$. The mobile phase velocity, u_m, is assumed to be constant and is not included in the differential.

$$\frac{\partial m}{\partial t} + u_m \frac{\partial}{\partial z}\left(\frac{m}{1+k}\right) = 0 \tag{A3}$$

Because the retention factor remains in the differential, the effect of the change in analyte velocity along the column length is captured in this approach. The two differential terms are substituted with the following finite difference equations

$$\frac{\partial m}{\partial t} = \frac{m_{z,t} - m_{z,t-1}}{\Delta t} \tag{A4}$$

$$\frac{\partial m}{\partial z} = \frac{m_{z,t-1} - m_{z-1,t-1}}{\Delta z} \tag{A5}$$

Solving for $m_{z,t}$ by letting $u_m = \Delta z/\Delta t$ (uniform mobile phase velocity) and using retention factors specific for each time and position results in

$$m_{z,t} = m_{z,t-1}\left(\frac{k_{z,t-1}}{1+k_{z,t-1}}\right) + m_{z-1,t-1}\left(\frac{1}{1+k_{z-1,t-1}}\right) \tag{A6}$$

This equation differs from that provided by Czok and Guiochon

$$m_{z,t} = m_{z,t-1}\left(\frac{k_{z,t-1}}{1+k_{z,t}}\right) + m_{z-1,t-1}\left(\frac{1}{1+k_{z,t}}\right) \tag{A7}$$

We believe this is because they did not account for the distance dependence of the analyte velocity in equation A2. While Czok and Guiochon's formulation gave reasonable accuracy for peak retention times and widths, mass balance was not conserved with their formulation, and peak areas were incorrect, which caused us to investigate eq. A7 in more detail, and to find the correct formulation, as represented by eq. A6. Equation A6 gives accurate peak areas for all conditions tested by us to date.

In the model used here, the time vector at $z = L$ (from the time/space matrix) is taken as the time-based chromatogram, in the sense that each element of this vector at a given z,t coordinate contains the mass of analyte that passes to the detector. However, from a physical point of view, the only analyte mass that can pass to the detector (m_d) is the mass in the mobile phase (m_m) – this is inconsistent with the fact that the model does not explicitly differentiate between the mass in the mobile and stationary phases (*i.e.*, see the two components on the right-hand side of eq. A6). Thus, the fraction of mass that is actually in the mobile phase at any time point in the chromatogram, $m_{L,t}$, must be calculated to produce a chromatogram with accurate peak heights and areas. These ideas are expressed by eq A7, where we recognize that the total mass at any $m_{L,t}$ is the sum of masses in the mobile (m_m) and stationary (m_s) phases (and that $m_d = m_m$), and recognize that m_s is the product of m_m and the retention factor at elution (k_e).

$$m_{L,t} = m_m + m_s = m_d + k_e m_d = m_d(1+k_e) \tag{A8}$$

$$m_d = \frac{m_{L,t}}{1+k_e} \tag{A9}$$

Appendix A. Supplementary data

Supplementary data associated with this article can be found, in the online version, at http://dx.doi.org/10.1016/j.chroma.2016.06.016.

References

[1] L.R. Snyder, J.J. Kirkland, J.L. Glajch, Practical HPLC Method Development, 2nd ed., Wiley Interscience, New York, 2012.
[2] J.W. Dolan, D.C. Lommen, L.R. Snyder, DryLab computer simulation for high-performance liquid chromatographic method development. II. Gradient elution, J. Chromatogr. 485 (1989) 91–112, http://dx.doi.org/10.1016/S0021-9673(01)89134-2.
[3] I. Molnar, Computerized design of separation strategies by reversed-phase liquid chromatography: development of DryLab software, J. Chromatogr. A 965 (2002) 175–194, http://dx.doi.org/10.1016/S0021-9673(02)00731-8.
[4] A.P. Schellinger, Y. Mao, P.W. Carr, Use of DRYLAB to compare octadecylsilane and carbon supports for reversed-phase chromatography of triazine herbicide test solutes, Anal. Bioanal. Chem. 373 (2002) 587–594, http://dx.doi.org/10.1007/s00216-002-1355-2.
[5] ChromSword Off-line (2015).
[6] J.W. Dolan, L.R. Snyder, M.A. Quarry, Computer simulation as a means of developing an optimized reversed-phase gradient-elution separation, Chromatographia 24 (1987) 261–276, http://dx.doi.org/10.1007/BF02688488.
[7] J.E. Eble, R.L. Grob, P.E. Antle, L.R. Snyder, Simplified description of high-performance liquid chromatographic separation under overload conditions, based on the Craig distribution model. I. Computer simulations for a single elution band assuming a Langmuir isotherm, J. Chromatogr. 384 (1987) 25–44, http://dx.doi.org/10.1016/S0021-9673(01)94659-X.
[8] S. Fasoula, C. Zisi, H. Gika, A. Pappa-Louisi, P. Nikitas, Retention prediction and separation optimization under multilinear gradient elution in liquid chromatography with microsoft excel macros, J. Chromatogr. A 1395 (2015) 109–115, http://dx.doi.org/10.1016/j.chroma.2015.03.068.
[9] L. Wang, J. Zheng, X. Gong, R. Hartman, V. Antonucci, Efficient HPLC method development using structure-based database search, physico-chemical prediction and chromatographic simulation, J. Pharm. Biomed. Anal. 104 (2015) 49–54, http://dx.doi.org/10.1016/j.jpba.2014.10.032.
[10] M. Czok, G. Guiochon, The physical sense of simulation models of liquid chromatography: Propagation through a grid or solution of the mass balance equation? Anal. Chem. 62 (1990) 189–200, http://dx.doi.org/10.1021/ac00201a020.
[11] K. Horváth, J.N. Fairchild, K. Kaczmarski, G. Guiochon, Martin-Synge algorithm for the solution of equilibrium-dispersive model of liquid chromatography, J. Chromatogr. A 1217 (2010) 8127–8135, http://dx.doi.org/10.1016/j.chroma.2010.10.035.
[12] K. Kaczmarski, D. Antos, Modified Rouchon and Rouchon-like algorithms for solving different models of multicomponent preparative chromatography, J.

Chromatogr. A 756 (1996) 73–87, http://dx.doi.org/10.1016/S0021-9673(96)00584-5.
[13] G.L. Frey, E. Grushka, Numerical solution of the complete mass balance equation in chromatography, Anal. Chem. 68 (1996) 2147–2154, http://dx.doi.org/10.1021/ac960220o.
[14] A. Felinger, Critical peak resolution in multicomponent chromatograms, Anal. Chem. 69 (1997) 2976–2979, http://dx.doi.org/10.1021/ac970241y.
[15] M.Z. El Fallah, G. Guiochon, Comparison of experimental and calculated results in overloaded gradient elution chromatography for a single-component band, Anal. Chem. 63 (1991) 859–867, http://dx.doi.org/10.1021/ac00020a010.
[16] M.Z. El Fallah, G. Guiochon, Gradient elution chromatography at very high column loading: effect of the deviation from the Langmuir model on the band profile of a single component, Anal. Chem. 63 (1991) 2244–2252, http://dx.doi.org/10.1021/ac00020a010.
[17] A. Felinger, G. Guiochon, Rapid simulation of chromatographic band profiles on personal computers, J. Chromatogr. A 658 (1994) 511–515, http://dx.doi.org/10.1016/0021-9673(94)80043-X.
[18] A.M. Katti, M. Czok, G. Guiochon, Prediction of single and binary profiles in overloaded elution chromatography using various semi-ideal models, J. Chromatogr. 556 (1991) 205–218, http://dx.doi.org/10.1016/S0021-9673(01)96222-3.
[19] L.R. Snyder, J.W. Dolan, D.C. Lommen, Drylab computer simulation for high-performance liquid chromatographic method development I. isocratic elution, J. Chromatogr. A 485 (1989) 65–89, http://dx.doi.org/10.1016/S0021-9673(01)89133-0.
[20] ACD/LC & GC Simulator—Model and Optimize LC and GC Separation Methods (2015).
[21] K.P. Xiao, Y. Xiong, F.Z. Liu, A.M. Rustum, Efficient method development strategy for challenging separation of pharmaceutical molecules using advanced chromatographic technologies, J. Chromatogr. A 1163 (2007) 145–156, http://dx.doi.org/10.1016/j.chroma.2007.06.027.
[22] L.R. Snyder, J.W. Dolan, High-Performance Gradient Elution: The Practical Application of the Linear-Solvent-Strength Model, Wiley, New York, NY, 2006.
[23] L.M. Blumberg, Theory of gradient elution liquid chromatography with linear solvent strength: part 1. Migration and elution parameters of a solute band, Chromatographia 77 (2013) 179–188, http://dx.doi.org/10.1007/s10337-013-2555-y.
[24] T. Baczek, R. Kaliszan, Computer assisted optimization of reversed-phase HPLC isocratic separations of neutral compounds, LCGC Eur. (2001) 2–6.
[25] Z. Ma, G. Guiochon, Application of orthogonal collocation on finite elements in the simulation of non-linear chromatography, Comput. Chem. Eng. 15 (1991) 415–426, http://dx.doi.org/10.1016/0098-1354(91)87019-6.
[26] G. Guiochon, A. Felinger, D.G. Shirazi, A.M. Katti, Single-component profiles with the equilibrium dispersive model, in: Fundamentals Preparative Nonlinear Chromatography, 2nd ed., Elsevier, B.V., Amsterdam, 2006, pp. 471–529.
[27] W. Hao, B. Di, B. Yue, Q. Chen, S. Wu, P. Zhang, Equivalence between the equilibrium dispersive and the transport model in describing band broadening in analytical gradient liquid chromatography, J. Chromatogr. A 1369 (2014) 191–195, http://dx.doi.org/10.1016/j.chroma.2014.10.015.
[28] J.E. Eble, R.L. Grob, P.E. Antle, L.R. Snyder, Simplified description of high-performance liquid chromatographic separation under overload conditions, based on the craig distribution model. II. Effect of isotherm type and experimental verification of computer simulations for a single band, J. Chromatogr. 384 (1987) 45–79, http://dx.doi.org/10.1016/S0021-9673(01)94660-6.
[29] J.E. Eble, R.L. Grob, P.E. Antle, L.R. Snyder, Simplified description of high-performance liquid chromatographic separation under overload conditions, based on the craig distribution model. III. Computer simulations for two co-eluting bands assuming a Langmuir isotherm, J. Chromatogr. 405 (1987) 1–29, http://dx.doi.org/10.1016/S0021-9673(01)81745-3.
[30] G. Vivo, S. Van Der Wal, P.J. Schoenmakers, G. vivó-Truyols, S. van der Wal, Comprehensive study on the optimization of online two-dimensional liquid chromatographic systems considering losses in theoretical peak capacity in first- and second-dimensions: a pareto-optimality approach, Anal. Chem. 82 (2010) 8525–8536.
[31] D.R. Stoll, K. O'Neill, D.C. Harmes, Effects of pH mismatch between the two dimensions of reversed-phase × reversed-phase two-dimensional separations on second dimension separation quality for ionogenic compounds—I. Carboxylic acids, J. Chromatogr. A 1383 (2015) 25–34, http://dx.doi.org/10.1016/j.chroma.2014.12.054.
[32] P.J. Schoenmakers, G. Vivó-Truyols, W.M.C. Decrop, A protocol for designing comprehensive two-dimensional liquid chromatography separation systems, J. Chromatogr. A 1120 (2006) 282–290, http://dx.doi.org/10.1016/j.chroma.2005.11.039.
[33] A.P. Schellinger, P.W. Carr, A practical approach to transferring linear gradient elution methods, J. Chromatogr. A 1077 (2005) 110–119, http://dx.doi.org/10.1016/j.chroma.2005.04.088.
[34] P.J. Schoenmakers, H.A.H. Billiet, R. Tijssen, L. De Galan, Gradient selection in reversed-phase chromatography, J. Chromatogr. 149 (1978) 519–537, http://dx.doi.org/10.1016/S0021-9673(00)81008-0.
[35] L.M. Blumberg, Theory of gradient elution liquid chromatography with linear solvent strength: part 2. Peak width formation, Chromatographia 77 (2013) 189–197, http://dx.doi.org/10.1007/s10337-013-2556-x.
[36] U.D. Neue, H.-J. Kuss, Improved reversed-phase gradient retention modeling, J. Chromatogr. A. 1217 (2010) 3794–3803, http://dx.doi.org/10.1016/j.chroma.2010.04.023.
[37] A. Vaast, E. Tyteca, G. Desmet, P.J. Schoenmakers, S. Eeltink, Gradient-elution parameters in capillary liquid chromatography for high-speed separations of peptides and intact proteins, J. Chromatogr. A 1355 (2014) 149–157, http://dx.doi.org/10.1016/j.chroma.2014.06.010.
[38] A. Vaast, E. Tyteca, G. Desmet, P.J. Schoenmakers, S. Eeltink, Corrigendum to gradient-elution parameters in capillary liquid chromatography for high-speed separations of peptides and intact proteins, J. Chromatogr. A 1355 (2014) 149–157, http://dx.doi.org/10.1016/j.chroma.2014.06.010.
[39] T. Raglione, S.A. Tomellini, T.R. Floyd, N. Sagliano, R.A. Hartwick, Zone compression effects in high-performance liquid chromatography, J. Chromatogr. 367 (1986) 293–300, http://dx.doi.org/10.1016/S0021-9673(00)94850-7.
[40] S. Keunchkarian, M. Reta, L. Romero, C. Castells, Effect of sample solvent on the chromatographic peak shape of analytes eluted under reversed-phase liquid chromatogaphic conditions, J. Chromatogr. A 1119 (2006) 20–28, http://dx.doi.org/10.1016/j.chroma.2006.02.006.
[41] C.B. Castells, R.C. Castells, Peak distortion in reversed-phase liquid chromatography as a consequence of viscosity differences between sample solvent and mobile phase, J. Chromatogr. A 805 (1998) 55–61, http://dx.doi.org/10.1016/S0021-9673(98)00042-9.
[42] P. Jandera, T. Hájek, P. Cesla, Effects of the gradient profile, sample volume and solvent on the separation in very fast gradients, with special attention to the second-dimension gradient in comprehensive two-dimensional liquid chromatography, J. Chromatogr. A 1218 (2011) 1995–2006, http://dx.doi.org/10.1016/j.chroma.2010.10.095.
[43] B.J. VanMiddlesworth, J.G. Dorsey, Quantifying injection solvent effects in reversed-phase liquid chromatography, J. Chromatogr. A 1236 (2012) 77–89, http://dx.doi.org/10.1016/j.chroma.2012.02.075.
[44] N.E. Hoffman, S.-L. Pan, A.M. Rustum, Injection of eluites in solvents stronger than the mobile phase in reversed-phase liquid chromatography, J. Chromatogr. 465 (1989) 189–200, http://dx.doi.org/10.1016/S0021-9673(01)92657-3.
[45] N.E. Hoffman, A. Rahman, Computation of band shape for strong injection solvent and weak mobile phase combinations in liquid chromatography, J. Chromatogr. 473 (1989) 260–266, http://dx.doi.org/10.1016/S0021-9673(00)91307-4.
[46] P.G. Stevenson, D.N. Bassanese, X.A. Conlan, N.W. Barnett, Improving peak shapes with counter gradients in two-dimensional high performance liquid chromatography, J. Chromatogr. A 1337 (2014) 147–154, http://dx.doi.org/10.1016/j.chroma.2014.02.051.
[47] D.R. Stoll, E.S. Talus, D.C. Harmes, K. Zhang, Evaluation of detection sensitivity in comprehensive two-dimensional liquid chromatography separations of an active pharmaceutical ingredient and its degradants, Anal. Bioanal. Chem. 407 (2015) 265–277, http://dx.doi.org/10.1007/s00216-014-8036-9.
[48] J. Layne, T. Farcas, I. Rustamov, F. Ahmed, Volume-load capacity in fast-gradient liquid chromatography: effect of sample solvent composition and injection volume on chromatographic performance, J. Chromatogr. A. 913 (2001) 233–242, http://dx.doi.org/10.1016/S0021-9673(00)01199-7.
[49] S.R. Groskreutz, A.R. Horner, S.G. Weber, Temperature-based on-column solute focusing in capillary liquid chromatography reduces peak broadening from pre-column dispersion and volume overload when used alone or with solvent-based focusing, J. Chromatogr. A 1405 (2015) 133–139, http://dx.doi.org/10.1016/j.chroma.2015.05.071.
[50] Y. Dai, G. Li, A. Rajendran, Peak distortions arising from large-volume injections in supercritical fluid chromatography, J. Chromatogr. A 1392 (2015) 91–99, http://dx.doi.org/10.1016/j.chroma.2015.02.063.
[51] J.N. Fairchild, J.F. Hill, P.C. Iraneta, Influence of sample solvent composition for SFC separations, LC-GC North Am. 31 (2013) 326–333.
[52] M. Enmark, D. Asberg, A. Shalliker, J. Samuelsson, T. Fornstedt, A closer study of peak distortions in supercritical fluid chromatography as generated by the injection, J. Chromatogr. A 1400 (2015) 131–139, http://dx.doi.org/10.1016/j.chroma.2015.04.059.
[53] D. Asberg, M. Lesko, M. Enmark, J. Samuelsson, K. Kaczmarski, T. Fornstedt, Fast estimation of adsorption isotherm parameters in gradient elution preparative liquid chromatography. I: The single component case, J. Chromatogr. A 1299 (2013) 64–70, http://dx.doi.org/10.1016/j.chroma.2013.05.041.
[54] D. Asberg, M. Lesko, M. Enmark, J. Samuelsson, K. Kaczmarski, T. Fornstedt, Fast estimation of adsorption isotherm parameters in gradient elution preparative liquid chromatography II: The competitive case, J. Chromatogr. A 1314 (2013) 70–76, http://dx.doi.org/10.1016/j.chroma.2013.09.003.
[55] V.C. Dewoolkar, L.N. Jeong, D.W. Cook, K.M. Ashraf, S.C. Rutan, M.M. Collinson, Amine gradient stationary phases on in-house built monolithic columns for liquid chromatography, Anal. Chem. 88 (2016) 5941–5949, http://dx.doi.org/10.1021/acs.analchem.6b00895.
[56] L.M. Blumberg, T.A. Berger, Variance of a zone migrating in a non-uniform time-invariant linear medium, J. Chromatogr. A 596 (1992) 1–13, http://dx.doi.org/10.1016/0021-9673(92)80197-3.
[57] L.M. Blumberg, Variance of a zone migrating in a linear medium. II. Time-varying non-uniform medium, J. Chromatogr. 637 (1993) 119–128, http://dx.doi.org/10.1016/0021-9673(93)83204-6.